Article

Immunity

Innate Lymphoid Cells Are Depleted Irreversibly during Acute HIV-1 Infection in the Absence of Viral Suppression

Graphical Abstract

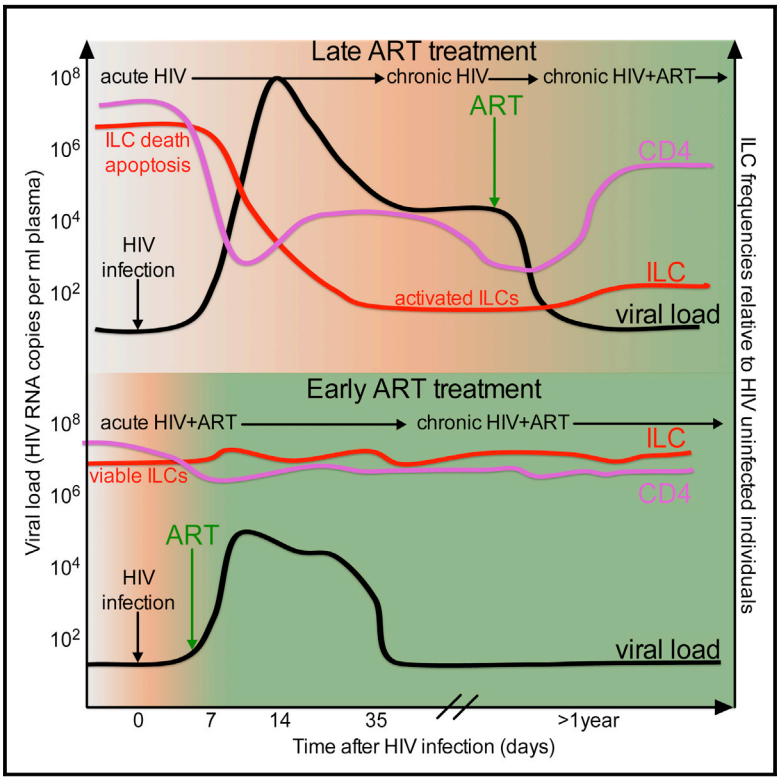

Authors

Henrik N. Kløverpris, Samuel W. Kazer, Jenny Mjösberg, ..., Bruce D. Walker, Thumbi Ndung'u, Alasdair Leslie

Correspondence

henrik.kloverpris@k-rith.org

In Brief

The impact of HIV-1 on ILCs remains unknown. Kløverpris and colleagues find that ILCs are rapidly depleted from the blood of HIV-1-infected individuals during acute infection. Antiretroviral therapy initiated during acute infection but not chronic infection prevents the loss of blood ILCs, suggesting that early treatment might preserve immune homeostasis.

Highlights

- ILCs are depleted from the blood during early acute HIV-1 infection
- Antiretroviral therapy initiated in acute, but not chronic, infection preserves ILCs
- RNA sequencing of ILCs during acute infection implicates apoptosis in their depletion
- Remaining ILCs in chronic disease are activated but do not migrate to tissue sites

Accession Numbers

GSE77088

Kløverpris et al., 2016, Immunity *44*, 391–405
February 16, 2016
http://dx.doi.org/10.1016/j.immuni.2016.01.006

Immunity
Article

Innate Lymphoid Cells Are Depleted Irreversibly during Acute HIV-1 Infection in the Absence of Viral Suppression

Henrik N. Kløverpris,[1,2,*] Samuel W. Kazer,[3,4,5,6] Jenny Mjösberg,[7] Jenniffer M. Mabuka,[1] Amanda Wellmann,[1] Zaza Ndhlovu,[8] Marisa C. Yadon,[1] Shepherd Nhamoyebonde,[1] Maximilian Muenchhoff,[8,9] Yannick Simoni,[10] Frank Andersson,[11] Warren Kuhn,[12] Nigel Garrett,[13,14] Wendy A. Burgers,[15] Philomena Kamya,[3,8] Karyn Pretorius,[8] Krista Dong,[3] Amber Moodley,[3] Evan W. Newell,[10] Victoria Kasprowicz,[1] Salim S. Abdool Karim,[14,16] Philip Goulder,[8,9] Alex K. Shalek,[3,4,5,6,17] Bruce D. Walker,[3,8,18] Thumbi Ndung'u,[1,3,8,19] and Alasdair Leslie[1,3]

[1]KwaZulu-Natal Research Institute for Tuberculosis & HIV (K-RITH), University of KwaZulu-Natal (UKZN), 4001 Durban, South Africa
[2]Department of Immunology and Microbiology, University of Copenhagen, 2200 Copenhagen, Denmark
[3]Ragon Institute of Massachusetts General Hospital, Massachusetts Institute of Technology and Harvard University, Cambridge, MA 02139-4307, USA
[4]Department of Chemistry, Massachusetts Institute of Technology, Cambridge, MA 02139-4307, USA
[5]Institute for Medical Engineering & Science, Massachusetts Institute of Technology, Cambridge, MA 02139-4307, USA
[6]Broad Institute of MIT and Harvard, Cambridge, MA 02139-4307, USA
[7]Center for Infectious Medicine, Karolinska Institute, 171 76 Stockholm, Sweden
[8]HIV Pathogenesis Programme, Doris Duke Medical Research Institute, UKZN, 4001 Durban, South Africa
[9]Department of Paediatrics, University of Oxford, Oxford OX1 3SY, UK
[10]Agency for Science, Technology and Research (A*STAR), Singapore Immunology Network (SIgN), 138632 Singapore, Singapore
[11]Department of Surgery, Inkosi Albert Luthuli Hospital, KwaZulu-Natal, 4058 Durban, South Africa
[12]ENT department Stanger Hospital, Stanger, KwaZulu Natal, 4450 Durban, South Africa
[13]Department of Infectious Diseases, UKZN, 4001 Durban, South Africa
[14]Center for the AIDS Programme of Research in South Africa – CAPRISA, 4001 Durban, South Africa
[15]Division of Medical Virology and Institute of Infectious Disease and Molecular Medicine, University of Cape Town, 7925 Cape Town, South Africa
[16]Department of Epidemiology, Columbia University, New York, NY 10027, USA
[17]Division of Health Sciences and Technology, Harvard Medical School, Boston, MA 02138, USA
[18]Howard Hughes Medical Institute, Chevy Chase, MD 20815, USA
[19]Max Planck Institute for Infection Biology, 10117 Berlin, Germany
*Correspondence: henrik.kloverpris@k-rith.org
http://dx.doi.org/10.1016/j.immuni.2016.01.006

SUMMARY

Innate lymphoid cells (ILCs) play a central role in the response to infection by secreting cytokines crucial for immune regulation, tissue homeostasis, and repair. Although dysregulation of these systems is central to pathology, the impact of HIV-1 on ILCs remains unknown. We found that human blood ILCs were severely depleted during acute viremic HIV-1 infection and that ILC numbers did not recover after resolution of peak viremia. ILC numbers were preserved by antiretroviral therapy (ART), but only if initiated during acute infection. Transcriptional profiling during the acute phase revealed upregulation of genes associated with cell death, temporally linked with a strong IFN acute-phase response and evidence of gut barrier breakdown. We found no evidence of tissue redistribution in chronic disease and remaining circulating ILCs were activated but not apoptotic. These data provide a potential mechanistic link between acute HIV-1 infection, lymphoid tissue breakdown, and persistent immune dysfunction.

INTRODUCTION

Hallmarks of HIV-1 pathology include immunodeficiency, lymphoid tissue destruction, gut barrier breakdown, and systemic immune activation (Veazey et al., 1998). These features are only partially reversed by fully suppressive long-term antiretroviral therapy (ART) (Sanchez et al., 2015; Zeng et al., 2012). The underlying mechanisms remain unclear, presenting a serious barrier to the development of novel interventions to improve immune reconstitution in HIV-1-infected individuals. Recent studies suggest that the rapid depletion of interleukin 17 (IL-17)- and IL-22-producing $CD4^+$ T cells within gut-associated lymphocyte tissue (GALT) during acute infection (Schuetz et al., 2014) leads to gut epithelial breakdown, because IL-17 and IL-22 are the key cytokines in mucosal homeostasis. In fact, the most rapid and prolific producers of IL-17 and IL-22 in tissue are innate lymphoid cells (ILCs) rather than conventional Th17 and Th22 cells (Cella et al., 2009; Cupedo et al., 2009), prompting the question: what

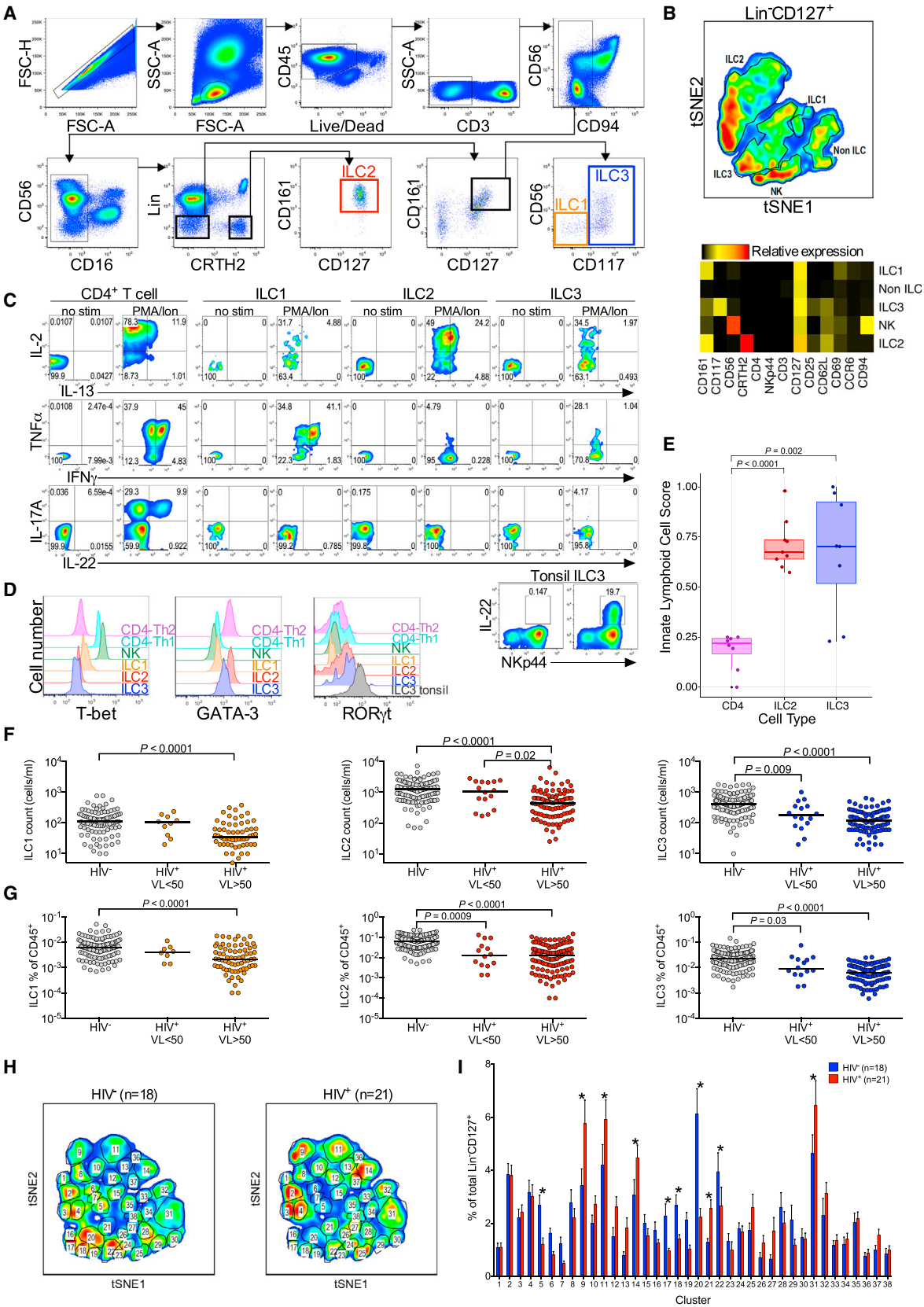

(legend on next page)

happens to this important immune subset after HIV-1 infection?

ILCs are not antigen specific and lack rearranged B and T cell receptors. ILCs are grouped into ILC1, ILC2, and ILC3, which share functional characteristics with Th1, Th2, and Th17 cells, respectively (Spits et al., 2013). ILCs respond rapidly to damage, prior to B and T cell expansion, and are therefore crucial for tissue homeostasis and repair during acute and chronic disease (McKenzie et al., 2014). In particular, ILCs are important in mucosal barrier maintenance through tissue repair, wound healing, and regulation of the immune response to commensals (Tait Wojno and Artis, 2012). As a result, ILCs are emerging as key players in many infectious and non-infectious diseases, where they can aid or impair proper immune response. Illustratively, group 2 ILCs (ILC2s) accumulate in the lung after influenza infection and restore epithelial integrity (Monticelli et al., 2011), and loss of gut ILC3s precipitates inflammatory bowel conditions through the IL-22 axis (Sonnenberg et al., 2012; Tait Wojno and Artis, 2012). In contrast, untreated multiple sclerosis, allergic asthma, and psoriasis are associated with expansions of ILCs in peripheral blood that might drive pathology (Bartemes et al., 2014; Perry et al., 2012; Teunissen et al., 2014).

The impact of HIV-1 on ILC populations in circulation and at mucosal barrier sites remains unclear. Given the central role of ILCs in gut epithelial integrity, immune regulation, and other systems dysregulated in HIV-1 disease, this represents a significant gap in our understanding of HIV-1 pathology.

In this study, we found that circulating ILCs were depleted 7–14 days after infection, in conjunction with an acute phase immune response. ILC numbers did not recover, in chronic infection, even with long-term fully suppressive ART. In contrast, we found that ILC populations were maintained if ART was started during early acute infection before peak viremia. We show that remaining ILCs circulating in chronic disease display an activated phenotype, but no direct evidence of apoptosis or migration to tissue sites. RNA sequencing of ILCs during early acute infection implicates apoptosis and cell death during ILC depletion. These gene signatures were diminished by early ART. Together these data suggest that depletion of circulating ILCs was mediated by cell death driven by high viral load (VL) during acute HIV-1 infection and associated with markers of acute viral response.

RESULTS

ILCs Are Depleted during Chronic HIV-1 Infection and Inversely Correlate with Viral Load Setpoint

ILCs are defined as lymphocytes that are negative for B and T cell lineage markers and conventional natural killer (NK) cell markers (CD16 and CD94) but positive for CD127 and CD161. Using flow cytometry of peripheral blood samples from HIV-1-infected and uninfected human donors, we adopted a traditional gating strategy and identified three phenotypically distinct ILC populations as described (Spits et al., 2013): $CRTH2^{-}CD117^{-}CD56^{-}CD25^{-/+}$ (ILC1), $CRTH2^{+}CD117^{-/+}CD56^{-}CD25^{-/+}$ (ILC2), and $CRTH2^{-}CD117^{+}CD56^{-/+}CD25^{-/+}$ (ILC3) (Figures 1A and S1A). To verify the identity of these three ILC populations, we turned to an unbiased data analysis tool, t-distributed stochastic neighbor embedding (tSNE), which simultaneously analyzes all flow-measured parameters, rather than sequentially gating. tSNE, like a principal-component analysis (PCA), clusters cells that share similar expression patterns together while accounting for potential nonlinear relationships between markers (Becher et al., 2014). With this approach, we identified five clusters within the lineage negative (Lin^{-}) $CD127^{+}$ population: ILC1, ILC2, ILC3, NK cell, and "non ILCs" that corresponded to the phenotypes of human ILCs (Figure 1B; Spits et al., 2013). To confirm the identity of these ILC subsets functionally, we performed intracellular cytokine staining, using $CD4^{+}$ T cells as a control, and, as expected, found mutually exclusive interferon-γ (IFN-γ) and IL-13 production from the ILC1 and ILC2 subsets, respectively (Figure 1C). The ILC3 subset in blood produced IL-2 and tumor necrosis factor α (TNF-α) but did not express NKp44 (not shown) and therefore did not secrete IL-22 (Teunissen et al., 2014). However, a high frequency of $NKp44^{+}$ ILC3s isolated from tonsil produced IL-22 (Figure 1C). In

Figure 1. Identification of Human ILCs from Blood Shows HIV-Specific Depletion of Circulating ILCs

(A) Representative conventional flow cytometry plots from an HIV-1-uninfected donor showing the hierarchical phenotype gating strategy from singlet lymphocytes to the ILC1 (orange), ILC2 (red), and ILC3 (blue) populations indicated by arrows and color-coded gates. Lineage (Lin) gate contains anti-CD3, CD4, CD11c, CD14, CD19, CD34, BDCA2, FcER1, TCR-αβ, and TCR-γδ antibodies.

(B) tSNE clustering of human PBMCs pre-gated for lymphocytes/singlets/live/$CD45^{+}/CD3^{-}/Lin^{-}/CD127^{+}$ that shows two-dimensional representation of high-dimensional space based on phenotype markers CD161, CD117, CD56, CRTH2, CD4, NKp44, CD25, CD62L, CD69, CCR6, and CD94 with gates indicating five identified clusters with heatmap showing the relative expression intensity for each marker within the five identified clusters (NK, ILC3, ILC1, "non-ILC," ILC2).

(C) Cytokine production after media or PMA/ionomycin stimulation from blood $CD4^{+}$ T cells, ILC1s, ILC2s, and ILC3s for six cytokines (IL-2, IL-13, IFN-γ, TNF-α, IL-17A, and IL-22) with tonsil-derived ILC3 shown as NKp44 versus IL-22.

(D) Transcription factor expression within $CD4^{+}$ Th2 cells (CRTH2 gated), $CD4^{+}$ Th1 cells (CD56 gated), NK cells ($CD3^{-}CD94^{+}CD56^{+}CD16^{+}$) ILC1, ILC2, and ILC3 for T-bet, GATA-3, and RORγt.

(E) Innate lymphoid cell score based on RNA-seq generated gene expression within $CD4^{+}$ T cell, ILC2, and ILC3 sorted populations from blood of nine HIV-uninfected individuals based on recently published gene transcripts of ILCs (Robinette et al., 2015).

(F) Absolute ILC counts for HIV-1-uninfected (n = 136), HIV-1-infected with undetectable plasma virus (VL < 50) (n = 16), and HIV-1-infected individuals with detectable viremia (VL > 50) (n = 91).

(G) ILC frequency expressed as percent of $CD45^{+}$ lymphotyces for HIV-1-uninfected (n = 122), HIV-1-infected with undetectable plasma virus (VL < 50) (n = 14), and HIV-1-infected individuals with detectable viremia (VL > 50) (n = 115). p values by Dunn's test for multiple comparisons.

(H) Grouping of cells gated from lymphs/singlets/live/$CD45^{+}/CD3^{-}/Lin^{-}/CD127^{+}$ according to automatic (unbiased) cluster designation for accumulated data from 18 HIV-1-uninfected (left) and 21 HIV-1-infected subjects with each distinct cluster named by its unique number inside gates.

(I) Bar graph showing the mean percentage contribution from each cluster (x axis), corresponding to the tSNE plots in (H), to the overall $Lin^{-}CD127^{+}$ population with $p < 0.02$ indicated by asterisk and calculated by t test comparing HIV-1-uninfected (n = 18) and HIV-1-infected (n = 21) individuals. p values by Student's t test and Sidak-Bonferroni method for multiple comparisons.

See also Figures S1 and S2.

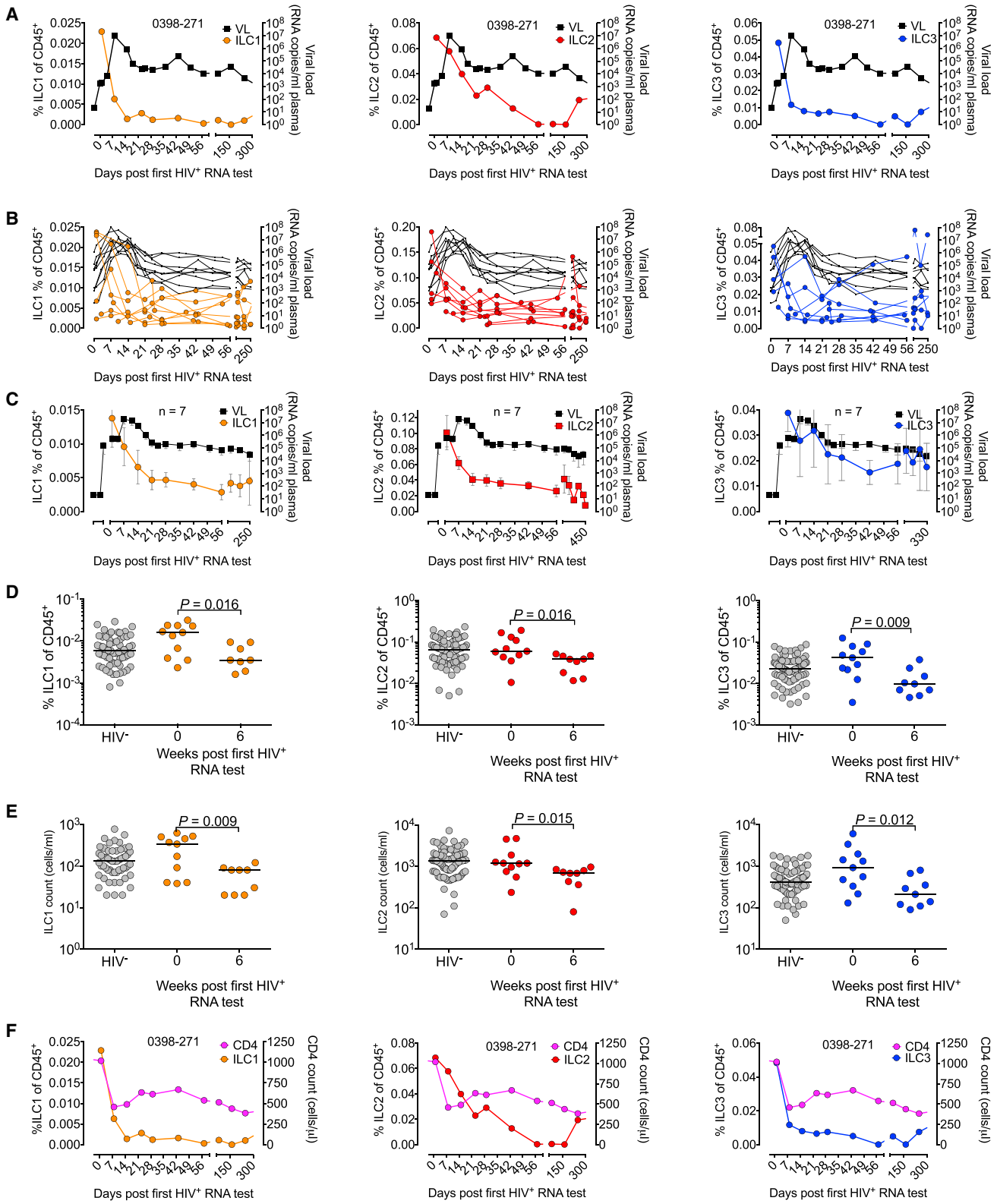

Figure 2. All ILC Populations Are Depleted during Early Acute HIV-1 Infection

(A) Data from the acutely HIV-1-infected subject (PID 0398-271) followed longitudinally over 10 time points from day 1 to day 249 from the day of first HIV+ RNA test, with ILC1s, ILC2s, and ILC3s shown as a percentage of the total CD45+ lymphocytes (left y axis, colored line) and the plasma VLs shown as HIV+ RNA copies/ml plasma (right y axis, black line).

(legend continued on next page)

addition, ILC subsets expressed the transcription factors T-bet, GATA-3, and RORγt in the expected patterns for the ILC1, ILC2, and ILC3 subsets, respectively, and relative to controls (conventional NK [T-bet] and CD4-Th1 [T-bet] and Th2 [GATA-3] cells) (Figure 1D; Spits et al., 2013). Finally, we performed RNA sequencing of sorted ILCs and $CD4^+$ T cells from the blood of nine healthy donors and found that the ILC populations displayed a distinct ILC transcriptional signature compared to sample-matched $CD4^+$ T cells (Figure 1E; Tables S1, S2, and S3). The ILC subsets themselves were closely related but transcriptionally distinct (Tables S1, S2, and S3), typified by expression of canonical ILC lineage genes, such as *CD117* (cKit; ILC3), *IL1R* (ILC3), and *KLRG1* (ILC2) (Figure S1B). Together, these data confirm the precise identification of the main human ILC subsets described.

Next, we compared the absolute number of blood ILCs in a total of 223 samples from HIV-1-uninfected, ART-naive viremic (HIV-1 RNA > 50 copies/ml plasma), and aviremic (<50 copies/ml) individuals with chronic HIV-1 infection (Figure 1F). In viremic subjects, we observed depletion of all three ILC populations ($p < 0.0001$). However, ILC1s and ILC2s, but not ILC3s ($p = 0.009$), were preserved in aviremic subjects (Figure 1F). ILC frequencies expressed as percentage of total $CD45^+$ lymphocytes confirmed their depletion during chronic HIV-1 (Figure 1G) and showed that changes in frequency of other hematopoietic subsets did not impact ILC measurements during chronic infection. In addition, we observed a significant negative correlation between HIV-1 RNA VL setpoint and ILC frequency ($p = 0.07$ to 0.007, $R = -0.18$ to -0.32) (Figures S2A and S2B), similar to the well-described correlation between VL and absolute $CD4^+$ T cell counts ($p < 0.001$, $R = -0.47$) (Figure S2C). Thus, ILCs are severely depleted in chronic viremic infection with a direct negative correlation to VL setpoint.

To examine shifts in ILC subsets driven by chronic HIV-1 infection, we used the tSNE algorithm (Becher et al., 2014) to obtain an unbiased analysis of ILC distribution. By gating on Lin^-CD127^+, we identified 38 distinct clusters with shared surface marker expression characteristics (Figure 1H). Ten of these clusters were significantly enriched or depleted in HIV-1-infected subjects (Figure 1I), predominantly from within the ILC2 and ILC3 populations. Of these, cluster 9 (ILC2) and cluster 20 (ILC3) remained significant after controlling for multiple comparisons ($p = 4.5 \times 10^{-5}$ and $p = 1.7 \times 10^{-11}$), suggesting that the circulating ILCs that remained during chronic HIV infection were phenotypically altered.

ILCs Are Depleted during Early Acute HIV-1 Infection

To further investigate the dynamics of ILC depletion, we turned to a unique acute HIV-1 infection cohort (Ndhlovu et al., 2015). Women in this cohort were tested for the presence of HIV-1 nucleic acid in plasma twice a week, and therefore HIV-1 infections were identified within a maximum of 4 days from their last negative test and approximately 5–14 days after transmission, corresponding to Feibig stage I (McMichael et al., 2010). We tracked ILC1s, ILC2s, and ILC3s in seven individuals throughout the course of peak viremia and into chronic infection (Figure 2). We found normal ILC frequencies at the first time points that were sampled before peak viremia but observed a rapid ILC depletion that coincided with the peak VL (days 7–14) (Figures 2B and 2C) and persisted without rebound into chronic infection ($p < 0.016$) (Figure 2D). This observation remained significant when we analyzed the absolute ILC counts (Figures 2E and S3A–S3C), demonstrating that ILC depletion is not a result of changes in the frequency of other subsets during this disease phase. In contrast, and as expected, the characteristic early nadir of absolute $CD4^+$ T cell count, temporally associated with peak viremia, rebounded rapidly, although to suboptimal levels (Figure 2F). Thus, these data show that the ILC depletion observed during chronic viremic infection occurred very early in the acute phase of infection and that, unlike $CD4^+$ T cells, ILCs failed to recover after the resolution of acute viremia to setpoint VL.

Early Depletion of ILCs Coincides with Spikes in Epithelial Gut Breakdown

ILCs are required to maintain an effective gut barrier and to regulate the immune response to commensal microbiota (Sonnenberg et al., 2012). We therefore next sought to define the kinetics of ILC decline in early acute HIV-1 infection in relation to the damage to gut-associated lymphoid tissue that occurs during primary infection in non-human primates (Veazey et al., 1998). Changes to gut integrity during acute HIV-1 infection were assessed indirectly by measuring the levels of intestinal fatty acid binding protein 1 (I-FABP), a plasma marker previously associated with gut barrier breakdown (Hunt et al., 2014). In one subject (PID 0398-271), we found a peak in I-FABP levels 1 week after ILC depletion and 2 weeks after HIV-1 plasma RNA detection (Figure S4A). When we compared the relative levels of I-FABP for the entire cohort, we consistently found maximum levels occurring 2 weeks after HIV-1 RNA detection that coincided with ILC depletion (Figure S4B). Although I-FABP levels return to baseline once VL reaches setpoint, the association between ILC levels and I-FABP was significant at 2 and 3 weeks after HIV-1 detection ($p < 0.008$) (Figure S4C), corresponding to 1 week after peak viral replication (Figure S4D). These data are consistent with the hypothesis that massive viral replication during acute infection leads to profound damage to the gut epithelial barrier and precipitates the well-described association between microbial translocation, immune activation, and disease progression. ILCs are central to gut epithelial repair, so the 4-fold increase in I-FABP levels and coincident loss of ILCs from circulation suggests a possible link, although this

(B) Data as shown in (A), but for the entire cohort (n = 7).
(C) Data as shown in (B), but cumulative data presented as mean values for the entire cohort (n = 7) with error bars showing SEM.
(D) Percentage ILC1s, ILC2s, and ILC3s of total $CD45^+$ lymphocytes shown for week 0 and week 6 after day of first HIV-1-positive test and compared to the HIV-uninfected subjects (n = 116).
(E) ILC frequencies expressed as absolute ILC counts shown for week 0 and week 6 after day of first HIV-1-positive test and compared to the HIV-uninfected subjects (n = 116).
(F) Data from the acutely HIV-1-infected subject (PID 0398-271) as shown in (A) but for absolute $CD4^+$ T cell counts (pink line, right y axis).
p values by Dunn's test for multiple comparisons. All samples are from "FRESH" cohort (Ndhlovu et al., 2015). See also Figures S2–S4.

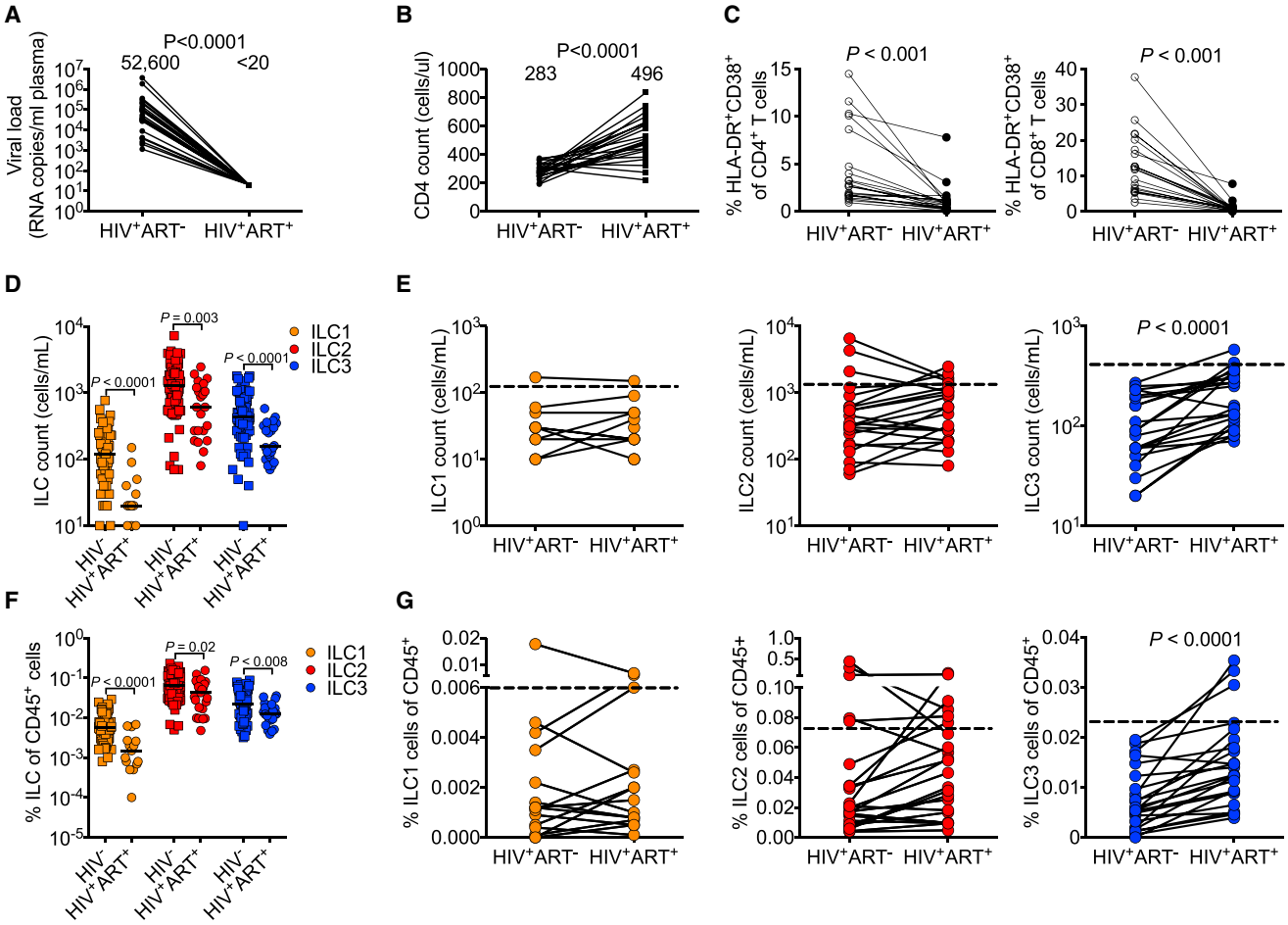

Figure 3. ILCs Are Not Reconstituted after Successful Treatment Initiated in Chronic Infection

Twenty-four individuals were tested every 3 months for the presence of early detectable HIV-1-specific p24 antibodies and followed over 9 years with average treatment initiation starting at median values of 213 weeks after infection and sampled again 2 years later.

(A) Median HIV-1 RNA copies/ml plasma before and after treatment.

(B) Absolute $CD4^+$ T cell counts.

(C) Percentage of $HLA\text{-}DR^+CD38^+$ expression gated on $CD4^+$ T cells and $CD8^+$ T cells before and after ART treatment.

(D) Absolute ILC counts comparing HIV-1-uninfected individuals (n = 81) to unmatched HIV-1-infected individuals (n = 22) with successful viral suppression after 2 years of treatment.

(E) Absolute ILC1, ILC2, and ILC3 counts from matched HIV-1-infected individuals before and after ART start (n = 22) with horizontal dotted line representing median absolute ILC counts for HIV-1-uninfected individuals.

(F) ILC frequencies expressed as percent of $CD45^+$ lymphocytes comparing HIV-1-uninfected individuals (n = 84) to unmatched HIV-1-infected individuals with successful viral suppression after 2 years of treatment (n = 22).

(G) Data as in (E) but expressed as percent ILCs of total $CD45^+$ lymphocytes.

p values by the Wilcoxon matched-paired signed rank test, Mann-Whitney U test and with correlation coefficients shown as spearman rank *r* and p values.

might be circumstantial and additional data are required to test this correlation.

ILC Depletion Is Irreversible despite Successful Suppression of Viremia by Antiretroviral Treatment in Chronic Infection

We next sought to investigate the relationship between ILC depletion and immune reconstitution after ART initiation. In a longitudinal treatment cohort (Abdool Karim et al., 2010), we measured ILC frequencies in chronically infected individuals at the last time point before ART initiation (median 213 weeks after infection) and 2 years into successful treatment (median 308 weeks after infection) (Figures 3A and 3B), as indicated by partial $CD4^+$ T cell reconstitution (Figure 3B) and reduced immune activation (Figure 3C). Unexpectedly, all three ILC populations failed to return to normal frequencies, and they remained significantly lower than in uninfected individuals despite undetectable VLs ($p < 0.02$) (Figures 3D–3G). Only blood ILC3s significantly rebounded with ART ($p < 0.0001$), but never to the frequencies observed in uninfected individuals (median 70 versus 430 ILC3s). There was no correlation between the recovery of ILCs and $CD4^+$ T cells in the same subjects ($p > 0.7$) (data not shown). Thus, the ILC depletion observed during both acute and chronic HIV-1 infection was irreversible when treatment was initiated in the chronic phase.

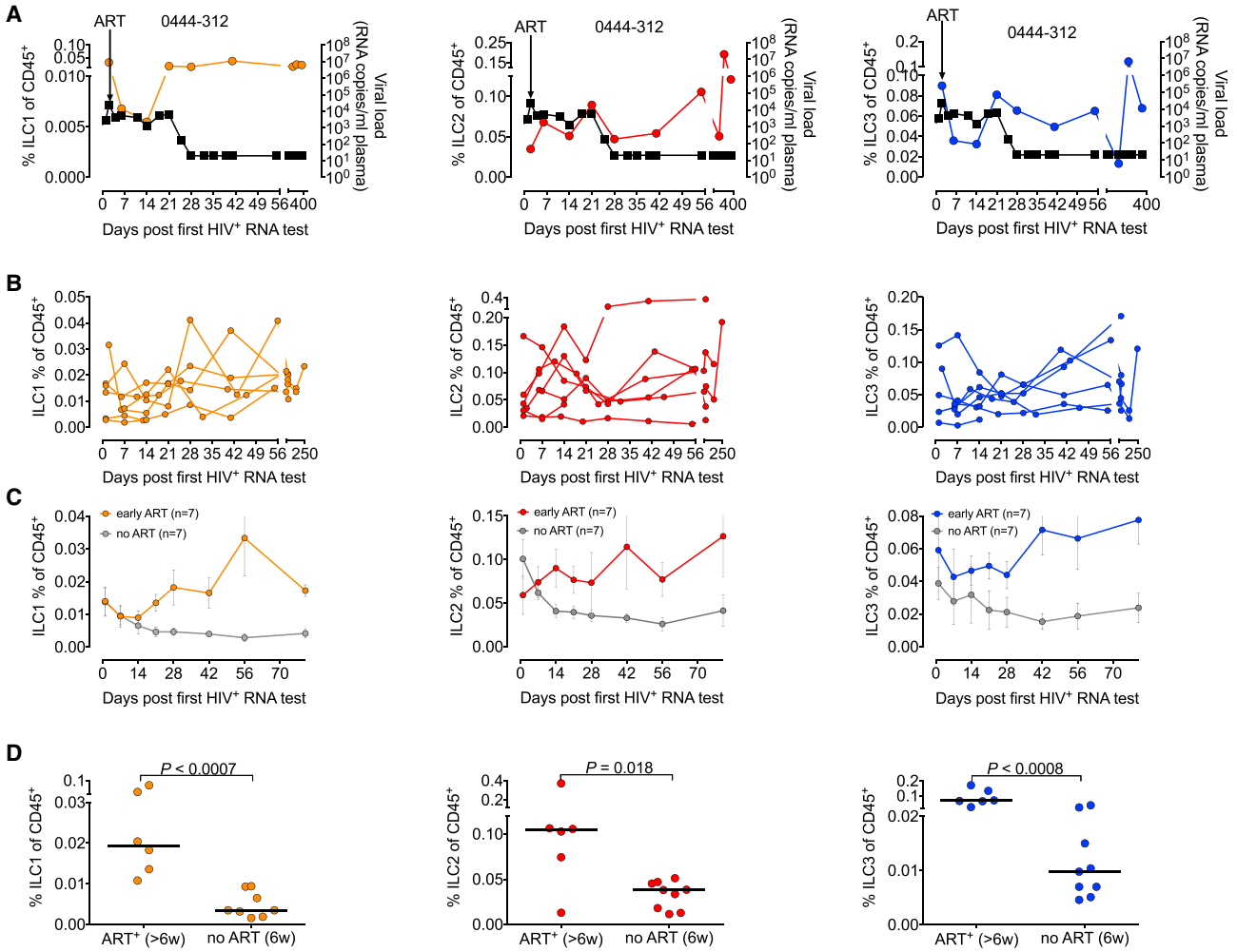

Figure 4. ILCs Are Preserved by Treatment Initiation during Early Acute HIV-1 Infection

(A) Data from one acute infected subject (FRESH cohort) that was treated 1 day after detection of HIV-1 RNA in plasma (VL = 2,900) as indicated by the black arrow and with ILC frequency shown as percent of CD45 lymphocytes tracked throughout 400 days after HIV-1 infection (left y axis) and with HIV-1 RNA copies/ml plasma (right y axis). ILC1, orange; ILC2, red; ILC3, blue; viral load indicated by black lines.

(B) Longitudinal data from seven acutely HIV-1-infected subjects initiated on ART within 1 day of plasma HIV-1 detection and shown as percent ILC of CD45 lymphocytes throughout acute infection.

(C) Longitudinal mean values comparing seven acutely infected individuals initiated on ART 1 day after HIV RNA detection (colored lines) to seven acutely infected individuals not receiving ART (gray lines) throughout 11 weeks after HIV detection with error bars representing SEM.

(D) ILC1, ILC2, and ILC3 frequencies for six acutely infected individuals receiving ART by day 1 of HIV detection (ART^+ individuals at >6 weeks after HIV detection) compared to nine treatment-naive acutely infected individuals from the same cohort 6 weeks into infection (no ART [6w]).

p values by Dunn's test for multiple comparisons.

ILC Depletion Is Prevented by Antiretroviral Treatment Initiated during Early Acute HIV-1 Infection

To investigate the potential capacity of ART initiated in early infection to reverse the negative impact of HIV-1 on circulating ILCs, we analyzed a unique subset of individuals in whom ART was initiated at the earliest possible time point: on the first day of HIV-1 RNA detection and within 5–14 days of HIV-1 transmission. From one subject (PID 0444-312), we observed reduced peak viremia, preserved $CD4^+$ T cells (871 before versus 745 cells/μl 4 weeks after infection), and no depletion of blood ILCs (Figure 4A). The preservation of ILCs relative to untreated subjects was consistent in all seven individuals receiving ART during early acute infection (Figure 4B) in contrast to acute infected individuals that did not receive treatment (Figure 4C). ILC frequencies in these subjects fluctuated to some extent during the course of acute infection but no clear patterns emerged. Whether this represents heterogeneity in the response of ILCs in these individuals to their ART or to natural variation is unclear. However, at >6 weeks into infection, all three ILC subsets were present at significantly higher frequencies than in untreated subjects ($p < 0.018$) (Figure 4D). Thus, ILC depletion during HIV-1 infection can be prevented by early ART.

ILC Depletion Associated with Signatures of Activation and Fas Upregulation

ILCs are unlikely to be directly infected by HIV-1 because they do not express the CD4 co-receptor and, in vitro, we were unable to

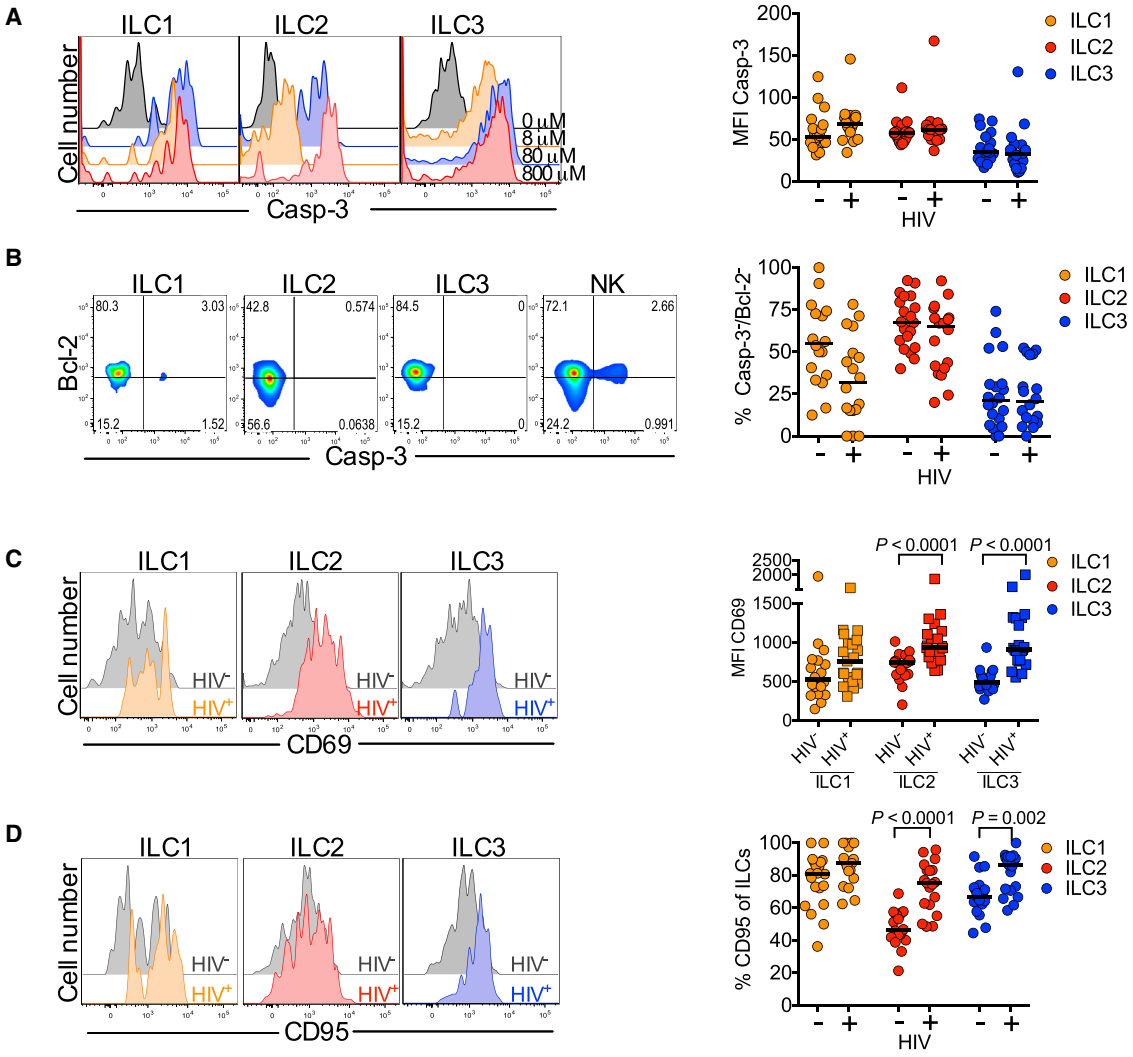

(legend on next page)

infect ILCs with HIV-1 using high titers of X4 and R5 virus (data not shown). In order to investigate alternative mechanisms of ILC depletion, we first measured the anti-apoptotic factor Bcl-2 and activated caspase-3, which are both involved in apoptosis. Although we were able to increase intensities of caspase-3 in all ILC subsets by incubation with the pro-apoptotic molecule camptothecin, we did not detect any significant changes in absolute (Figure 5A) or relative (Figure 5B) intensity of Bcl-2 or caspase-3 expression when comparing ILCs from HIV-1-uninfected and chronic infected subjects. As expected (Petrovas et al., 2004), we did detect elevated signatures of apoptosis in $CD8^+$ T cells from chronically infected individuals using this assay (data not shown).

We next examined the activation status of the remaining circulating ILCs after HIV-1 infection, because HIV-1-induced immune activation is implicated in $CD4^+$ T cell depletion (Brenchley et al., 2004). We found a significant increased surface expression of the lymphocyte activation marker CD69 on ILC2s and ILC3s ($p < 0.0001$) (Figure 5C) and on T cells (data not shown) in HIV-1-positive subjects, demonstrating activation of ILCs in response to infection. However, when we measured CD38, a marker of general immune activation on T cells, we found low expression levels on ILC1s, ILC2s, and ILC3s compared to $CD4^+$ and $CD8^+$ T cells, with no correlation to ILC frequencies in HIV-1-infected individuals (data not shown). In addition, we found no difference in CD38 expression on ILC1s, ILC2s, and ILC3s comparing infected and uninfected individuals in contrast to significant differences observed for both $CD4^+$ and $CD8^+$ T cells ($p < 0.01$) (data not shown), suggesting that different activation markers exist for ILCs and T cells in HIV-1 infection. We observed significant upregulation of the mucosal tissue homing receptors $\alpha4\beta7$, but only in the ILC3 subset (Figure S5A) and not in their T cell counterparts or in ILC1 and ILC2 subsets (data not shown).

Plasma IL-7 is known to be elevated in chronic HIV-1 infection (Hodge et al., 2011) and it is the ligand for CD127, a receptor that is expressed on all ILC subsets and is critical for their generation and maintenance (Spencer et al., 2014). Therefore, we next measured plasma levels of IL-7 by ELISA in matched samples and found a weak positive associations with the frequency of ILC1 and ILC2 and plasma IL-7 levels in HIV-1-infected individuals, but no association with ILC3s (Figure S5B). These data suggest that IL-7 does not play a role in persistent ILC depletion in chronic HIV-1 infection.

A recent study suggests that cell death protein Fas-FasL interactions are involved in ILC3 apoptosis in a humanized mouse model of HIV-1 (Zhang et al., 2015). Therefore, we measured the relative intensity of CD95 (Fas) expression in chronic HIV-1 and found significant upregulation on ILC2 and ILC3 subsets measured by percent CD95 expression (Figure 5D) and for the ILC1 subset by relative MFI ($p = 0.004$) (data not shown). The Fas-mediated apoptosis reported by Zhang et al. (2015) was driven by IFN-α, and we therefore looked to see whether the ILC depletion observed in our acute HIV-1 cohort correlated with plasma quantities of this cytokine, reported to be induced in this early phase of infection (Stacey et al., 2009). Plasma concentrations of IFN-α and the IFN-induced protein IP-10 were measured in samples from 2 to 12 weeks before infection (plotted as day −7) followed by 3, 7, 14, and 30 days after HIV-1 RNA detection. IP-10 was induced by primary viraemia (66%), confirming immune activation and the existence of a strong IFN signature associated with acute infection ($p = 0.038$) (Figure 5E). In addition, we observed a modest increase (11%) in IFN-α over baseline prior to peak viremia ($p = 0.077$) (Figure 5F). In the limited samples available ($n = 4$), we found that IP-10 concentrations were greatly reduced by immediate ART, consistent with a blunted IFN response, but the impact on IFN-α was not apparent (Figures 5E and 5F). These data are consistent with the hypothesis that ILC depletion is driven by immune activation during acute viraemia and prevented by early treatment, although the role of IFN-α specifically is not clear.

RNA-Seq Analysis Reveals Downregulation of Genes Associated with Cell Viability and Proliferation in ILCs Immediately after HIV-1 Infection

To gain a deeper understanding of ILC depletion in HIV-1 infection, we performed bulk RNA-seq on samples from early acute infection. RNA-seq is a sensitive and powerful method for determining changes in cell populations and behaviors (Rapaport et al., 2013). mRNA from $CD4^+$ T cells, ILC2s, and ILC3s isolated at various time points were sequenced from two untreated patients and two patients who started ART immediately after viral RNA detection. Transcriptional comparisons were made between both HIV detection and peak viremia and between peak viremia and 6 weeks after detection for each patient in order to generate lists of significantly differentially expressed genes (Figures 6A and S6A).

First, we compared viral detection and peak viremia to understand transcriptional changes in response to the antigenemia and cytokine response associated with this phase (McMichael et al., 2010). Both ILC2s and ILC3s in untreated patients showed

Figure 5. ILCs from Peripheral Blood of Chronic HIV-1-Infected Individuals Are Not Apoptotic but Display an Activated Phenotype and Upregulation of Fas

(A) Activated caspase-3 measured by median fluorescence intensity (MFI) after log fold titration of camptothecin at 0, 8, 80, and 800 μM shown for ILC1, ILC2, and ILC3 with cumulative data from MFI values for caspase-3 comparing 20 HIV-negative and 18 chronic HIV-positive individuals for ILC1, ILC2, and ILC3 subsets.

(B) One representative example of percentage Bcl-2- and caspase-3-negative ILC1, ILC2, ILC3, and NK ($CD3^-CD56^+CD94^+CD16^+$) cell subsets with cumulative data shown on the right as the percentage of $Bcl\text{-}2^-/casp\text{-}3^-$ cells of ILC1, ILC2, and ILC3 subsets.

(C) MFI expression for CD69 on ILC1s, ILC2s, and ILC3s comparing HIV-negative ($n = 18$) and chronic HIV-positive ($n = 21$) subjects.

(D) Fas (CD95) expression on ILC1, ILC2, and ILC3 gated cells overlayed by HIV-1 uninfected (gray) and HIV-1 infected (color) comparing 20 uninfected and 20 infected subjects (right).

(E) Plasma IP-10 mean levels (left y axis) shown for 14 acutely infected treatment-naive subjects sampled before infection (7–60 days prior to HIV detection plotted as day −7) followed 30 days into infection (left), and with four subjects treated 1 day after HIV-1 detection (right) and with plasma HIV RNA copies/ml levels shown on the right y axis.

(F) Same as for (E) but with data for IFN-$\alpha2$.

Error bars represent SEM values. p values by Mann-Whitney U test and paired t test. See also Figure S5.

A

Patient	Detection (Days)	VL Detection	Peak Viremia (Days)	VL Peak Viremia	6 Weeks (Days)	VL 6 Weeks
0450-318	1	160,000	7	1,400,000	38	790,000
0387-272	1	87,000	7	100,000,000	49	2,300
0629-453 (ART)	1	2,900	6	3,400	40	20
0444-312 (ART)	--	--	2	24,000	41	20

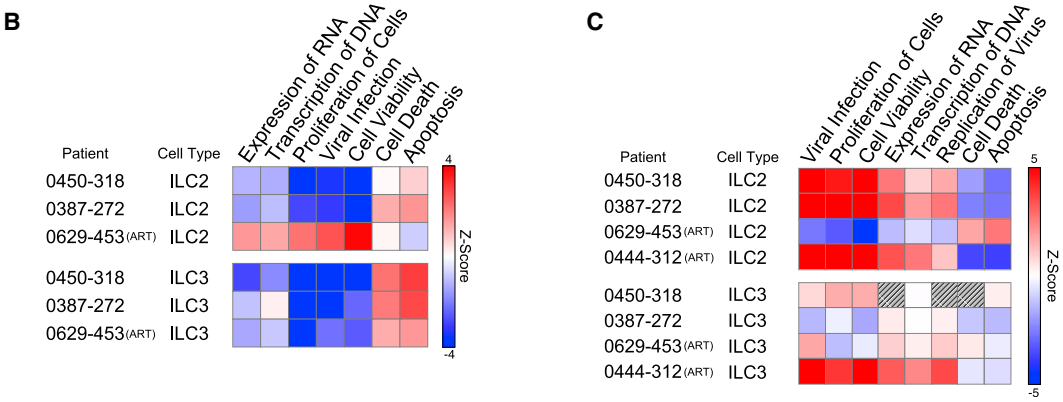

Figure 6. ILCs Show Upregulation of Genes Associated with Apoptosis and Cell Death in Early Acute HIV-1 Infection

RNA-seq was performed on samples from two untreated and two early ART-treated subjects (FRESH cohort) during the course of early acute HIV infection.

(A) Sampling points and associated VLs for each patient. NB: patient 0444-312 did not have a sample collected prior to peak VL.

(B) Heat map of activation z-scores for functionally enriched gene sets differentially expressed between initial viral detection and peak viremia.

(C) Similar plot comparing enrichments between peak viremia and approximately 6 weeks after detection. z-score was calculated using log fold change in expression values (see Experimental Procedures).

See also Figure S6.

statistically significant ($p < 0.01$) downregulation of genes associated with cell proliferation and viability and upregulation of those linked to apoptosis and cell death (Figures 6B and S6B, Table S4). These changes were less apparent in an early acute ART-treated patient (PID 0629-453), demonstrating a mitigated response to HIV infection. In addition, several key upstream immune regulators were found to change in ILC2s and ILC3s immediately after infection (Figure S6D). Although ILCs lack T cell receptor expression at the protein level, there were significant changes in genes associated with CD3, also reported in transcriptional profiling of ILCs in murine models (Robinette et al., 2015). However, we found no evidence of TCR gene modules and the role of these genes in ILCs is unclear.

We also compared transcriptional profiles of ILCs at peak viremia and approximately 6 weeks after infection to probe the state of the ILCs that survive acute infection. In contrast to early changes, we found that ILC2s from untreated patients displayed upregulated cell proliferation and cell viability and downregulated cell death and apoptosis (Figures 6C and S6C, Table S5). This was consistent with our flow cytometry data showing that ILCs persisting in chronic infection show no evidence of increased apoptosis or cell death. Additionally, although phenotypically skewed (see Figures 1H and 1I), the remaining ILCs show signs of typical cellular function and immune response (Figure S6E). The early ART-treated patients, on the other hand, show mixed responses after peak viremia. Thus, ILC2s and ILC3s, in the absence of early antiretroviral treatment, undergo cell death by apoptosis during peak viremia.

Tonsil- and Gut-Resident ILCs Are Not Enriched or Depleted in Chronic HIV-1 Infection

Current studies of the involvement of ILCs in disease have focused primarily on their effector function in lymphoid and non-lymphoid tissue such as lung, skin, and intestine (McKenzie et al., 2014). Therefore, to investigate how changes in circulating ILCs relate to lymphoid-tissue-resident cells, we next turned to tissue samples from HIV-1-infected and uninfected subjects. We first examined surgically removed tonsils, lymphoid organs that support HIV-1 replication and undergo profound tissue remodeling during progressive disease (Doitsh et al., 2014; Sanchez et al., 2015). We identified tissue-resident ILCs and confirmed these subsets by transcription factor staining in comparison to NK and $CD4^+$ Th2 cells (Figure 7A). We found higher frequencies of ILC1s and ILC3s, but not ILC2s, compared to the blood (Figure S7A), with a distinct $CD69^+$ and $CD62L^-$ phenotype (Figure 7B) that is characteristic of tissue-resident T lymphocytes. No significant depletion of $CD4^+$ T cells from the HIV-1-infected tonsils, known to be directly infected by the virus, was observed (Figure 7C; Doitsh et al., 2014). Interestingly, no significant effect of HIV-1 on ILC frequency, subtype, or phenotype in tonsil tissues was observed (Figures 7D and 7E), nor any differences of the apoptotic markers active caspase-3 and Bcl-2

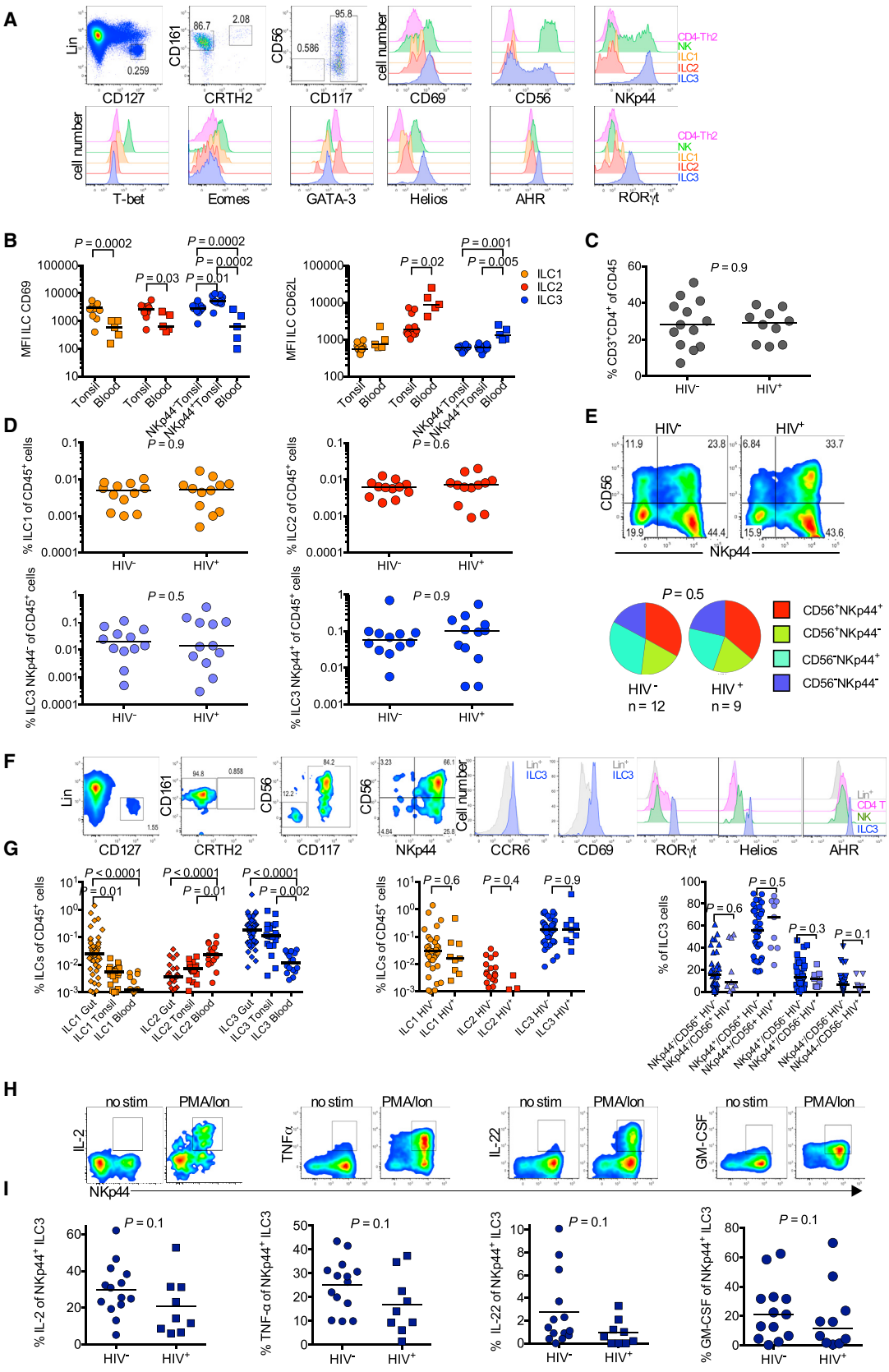

(legend on next page)

(data not shown), that might explain their loss from circulation. We next examined ILC frequencies in the gut mucosa, which is a major site of HIV-1 replication and $CD4^+$ T cell depletion (Mattapallil et al., 2005) and where ILC3s play a crucial role in homeostasis and barrier function. Using gut biopsies from subjects undergoing colonoscopy, we identified a distinct lineage-negative $CD127^+$ ILC population that was dominated by cKit-positive ILC3s expressing CD56, NKp44, CCR6, CD69, and transcription factors RORγt, Helios, and AHR (Figure 7F). In 46 subjects, we found increased levels of ILC1 and ILC3, but not ILC2, compared to tonsil and blood ($p < 0.0001$) (Figure 7G). However, we observed no differences in gut-resident ILC frequencies between HIV-1-infected ($n = 9$) and uninfected ($n = 37$) individuals, nor do we detect any difference in NKp44 and CD56 ILC3 phenotype (Figure 7G). Together these data provide no evidence that ILCs are either recruited to or depleted from lymph nodes or the gut mucosal barrier.

Finally, to assess the impact of HIV-1 on ILC function, we measured cytokine production in tonsil ILCs from infected and uninfected individuals, stimulated non-specifically with PMA and ionomycin. Cytokine production in these cells was restricted to $NKp44^+$ ILC3s (Figures 7H and S7B; $p < 0.0001$) and was dominated by IL-2, TNF-α, and GM-CSF and, to a lesser extent, IL-22. No IFN-γ or IL-13 was detected from $NKp44^+ROR\gamma t^+$ ILC3s (data not shown). Although a consistent trend was observed for decreased cytokine production in tonsil-resident ILC3s from HIV-1-infected individuals, these differences were not significant in the sample size obtained here. Taken together, ILC frequencies in tonsil and gut tissue from HIV-infected subjects did not support ILC redistribution from circulation.

DISCUSSION

The role of ILCs during chronic viral infection in humans remains unclear (Diefenbach, 2013), despite compelling evidence highlighting the importance of ILCs in immune regulation and mucosal barrier maintenance (Sonnenberg et al., 2012; Tait Wojno and Artis, 2012). Here, we report a rapid and irreversible depletion of blood ILCs during acute HIV-1 infection that persists in chronic infection in proportion to VL. During the chronic phase, ILC depletion is associated with altered subset composition and increased expression of activation (CD69) and tissue homing (α4β7) markers and the Fas death receptor (CD95). Upregulation of FAS makes ILC3s more susceptible to anti-CD95 antibody-induced apoptosis in vitro (Zhang et al., 2015); however, we detect no apoptotic ILCs ex vivo in chronic human HIV-1 infection measured either by caspase 3 activation or loss of bcl-2. In contrast, in early acute infection, we find that ILCs upregulate genes associated with cell death and apoptosis, potentially explaining their disappearance in the absence of early ART. This coincides with a strong IFN response induced by peak viral replication, demonstrated by the rapid elevation in plasma IP-10 and to a lesser extent IFN-α. We find no evidence of enrichment of tissue-resident ILCs in either tonsil or gut samples, suggesting that ILC depletion from circulation is explained by apoptosis rather than tissue redistribution.

Despite the correlation between VL and ILC levels in chronic infection, removal of viral burden and reduction of immune activation during this phase with fully suppressive ART does not restore circulating ILC populations. There is a partial rebound of ILC3s, but they remain well below the levels found in healthy donors. This suggests that sustained viremia leads to a fundamental impairment of the ILC arm of the immune system, which could have far-reaching immunological consequences (Marchetti et al., 2013). The role of acute viremia in ILC depletion is supported by data from patients in whom ART was initiated prior to peak viremia. In these individuals we observe no sustained depletion of ILCs and, in contrast to untreated individuals or those treated later, ILCs remain at the levels observed in uninfected individuals. This is associated with an absence of the transcriptional signature of apoptosis and the strong plasma IP-10 response observed in the untreated individuals. What role this early IFN response has in ILC depletion is not clear from our data, although IFN-α in particular has been implicated in ILC3 depletion in the humanized mouse model (Zhang et al., 2015). Importantly, depletion of ILCs from blood is not a general acute phase response to infection; filarial infection in humans is associated with expansion of blood ILCs (Boyd et al., 2014), suggesting the specific relevance of this phenomena to HIV-1. Indeed, more than 90% of individuals sampled from the same populations investigated here were infected with CMV and EBV (unpublished data), yet displayed normal blood ILC levels compared to individuals from areas without endemic viral infections (Munneke et al., 2014). In addition, direct infection of ILCs

Figure 7. Magnitude and Phenotype of Tissue-Resident ILCs Identified using Transcription Factors within Tonsil and Gut Tissue

(A) Gating of live $CD45^+CD3^-$ ILC1s ($Lin^-CD127^+CD161^+CRTH2^-CD117^-CD56^-$), ILC2s ($Lin^-CD127^+CD161^+CRTH2^+$), ILC3s ($Lin^-CD127^+CD161^{+-}CRTH2^-CD117^+CD56^{-/+}$), NK cells ($CD3^-CD94^+CD56^+$), and $CD4^+$ Th2 cells ($CD3^+CD4^+CRTH2^+$) and overlayed for CD69, CD56, and NKp44 expression and stained for T-bet, Eomes, GATA-3, Helios, AHR, and RORγt transcription factors.

(B) Median fluorescence intensity (MFI) of CD69 and CD62L expression on ILC1, ILC2, and ILC3 subsets in tonsil- and blood-resident T cells with $NKp44^{+/-}$ ILC3 subsets in tonsils (NKp44 not expressed in blood cells).

(C) Frequency of $CD4^+$ T cells shown as percent of $CD45^+$ cells within tonsil cells obtained from 12 HIV-uninfected and 10 HIV-infected subjects.

(D) Comparing ILC1, ILC2, and ILC3 subsets expressed as percent of $CD45^+$ lymphocytes in HIV-infected ($n = 12$) and uninfected ($n = 12$) individuals.

(E) ILC3 phenotype distribution of CD56- and NKp44-positive and -negative subsets with FACS plot showing one representative example and pie charts showing data for a total of 21 subjects.

(F) Gut-tissue-resident live $CD45^+CD3^-CD4^-$ lymphocytes gated as in (A) with ILC3s overlayed on Lin^+ ($CD45^+CD3^-Lin^+$) shown for CCR6 and CD69 and shown for RORγt, Helios, and AHR transcription factors for gut Lin^+, $CD4^+$ T, and NK cells and ILC3s.

(G) Cumulative data for ILC1, ILC2, and ILC3 frequencies expressed as percent of $CD45^+$ lymphocytes from gut, tonsil, and blood (left) with ILC1, ILC2, and ILC3 frequencies shown for 39 HIV-1-uninfected and 9 HIV-infected subjects (middle) and comparing ILC3 NKp44/CD56 phenotype expression from HIV-1-uninfected and -infected subjects (right).

(H and I) Intracellular cytokine staining after media or PMA/ionomycin stimulation for 5 hr shown for IL-2, TNF-α, IL-22, and GM-CSF production in $NKp44^+$ ILC3 gated cells (H) and with cumulative data shown in (I) obtained from HIV-1-infected ($n = 9$) and uninfected ($n = 14$) individuals.

p values by the Wilcoxon matched-paired signed rank test and Mann-Whitney U test with horizontal bars representing median values. See also Figure S7.

by HIV-1 is highly unlikely because they lack viral entry receptors consistent with resistance to high titered in vitro infection of either X5 or R4 virus.

Those ILCs that do survive peak viremia and persist in chronic infection show no evidence of apoptosis by protein expression (Bcl-2 and active caspase-3) and exhibit comparatively downregulated apoptosis and cell death transcription signatures by RNA-seq. In fact, genes associated with viral infection and immune response are upregulated in these populations, consistent with the measured increase in CD69 expression. Whether a certain subset of ILCs never initiates apoptosis in early acute infection or a population is consistently renewed at lower levels in the blood during chronic infection remains unclear.

In addition to apoptosis during acute infection, a potential mechanism for the depletion of circulating ILCs is that they home to major sites of HIV-1 replication and tissue damage. The fact that we detect no significant increase in ILCs within tonsil or gut tissue might be due to sensitivity. However, significant increases in ILC subsets are detectable in the livers of fibrotic mice (McHedlidze et al., 2013) and skin of human psoriasis sufferers (Teunissen et al., 2014). Furthermore, significant enrichment of NKp44$^+$ lineage-negative cells, which probably represent the ILC3 NKp44$^+$ subset, are observed in the tonsils of SIV-infected macaques (Reeves et al., 2011). Subsequent studies observed depletion of the ILC3 NKp44$^+$ subset from the GALT and mesenteric lymph nodes of acutely and chronically SIV-infected macaques (Li et al., 2014; Xu et al., 2015). Why an enrichment of NKp44$^+$ ILCs occurs in the tonsils of SIV-challenged monkeys and not in naturally infected human subjects remains unclear, but these data imply that either enrichment or depletion of ILCs in the context of retroviral infection would be possible to detect.

The fact that Li et al. (2014) observed a depletion of an ILC3-like subset from the GALT of acutely SIV-infected macaques is consistent with the depletion of circulating ILC3s we observe in acute HIV-1 infection and concomitant spike in I-FABP levels. The limited recovery of blood ILC3s observed after successful drug treatment suggests that this subset remains impaired and that continued immune activation might relate to the functional inability of gut-resident ILC3s in HIV-1-infected individuals (Zhang et al., 2015) to restore gut barrier integrity and prevent microbial translocation (Brenchley et al., 2004). Whether ILCs play a direct role in the HIV-1 pathology is difficult to study in human samples and therefore animal studies are warranted to elucidate the mechanistic details relating to the direct consequence of ILC depletion in HIV/SIV pathology (Reeves et al., 2011; Zhang et al., 2015). However, we believe that ILCs are likely to play an important role in HIV-1 pathology given the existence of an IL-22-producing NKp44$^+$ ILC3 subset that is required to both maintain the gut mucosa and limit the response to gut microbial contents (Cella et al., 2009; Sonnenberg et al., 2012). Irreversibly depleted ILC3s by HIV-1 infection would suggest a clear mechanism behind the continued immune activation observed even in individuals with successful long-term viral suppression by ART (Sanchez et al., 2015; Zeng et al., 2012), which is the strongest predictor for the onset of AIDS (Hunt et al., 2014).

In summary, we demonstrated that the persistent and irreversible ILC depletion that occurs immediately after HIV-1 acquisition correlates with disease stage and is not restored by long-term fully suppressive ART, but can be blocked by early treatment. This provides a potential mechanistic link between HIV-1 infection, lymphoid tissue breakdown, and persistent immune dysfunction that merits further exploration and suggests the importance of early ART administration in maintaining normal immune system composition and functionality.

EXPERIMENTAL PROCEDURES

Subjects

We used samples from a total of 122 HIV-1-uninfected subjects and 137 HIV-1-infected subjects. All participants were women with sub-Saharan Zulu/Xhosa ancestry from four independently collected cohorts within or in the greater area of Durban, KwaZulu-Natal, South Africa. All subjects provided informed consent and each study was approved by the respective institutional review boards including the Biomedical Research Ethics Committee of the University of KwaZulu-Natal for all the studies. See Supplemental Experimental Procedures for further information.

Clinical Parameters

VLs were obtained with the Roche Amplicor 1.5 assay (iThimba and CAPRISA002 cohorts) or the BioMerieux Nuclisens v2.0 (FRESH and GATEWAY cohorts) at Global Clinical and Viral Laboratories, Durban, South Africa. CD4$^+$ T cell counts and total lymphocyte counts were determined as previously described (Abdool Karim et al., 2010).

Flow Cytometry

We used different antibody panels for phenotype and transcription factor staining. See Supplemental Experimental Procedures for specific antibodies used throughout the study.

All samples were surface stained at room temperature for minimum 20 min and intracellularly stained at room temperature for at least 20 min. All samples were fixed in 2% paraformaldehyde before acquisition on a 4 laser, 17 parameter BD Fortessa flow cytometer within 24 hr of staining. Data were analyzed with FlowJo v.9.7.2 (TreeStar).

ELISA

Intestinal Fatty Acid Binding Protein (I-FABP) was measured using the ELISA kit human FABP2 DuoSet and R&D Systems and plasma IL-7 levels were measured using the recombinant human IL-7 kit from R&D Systems (cat# 207-iL). IFN-α and IP-10 were measured with the Milliplex kit (Millipore) and completed according to the manufacturer's protocol.

tSNE Analysis of Flow Cytometry Data

Unbiased representations of multi-parameter flow cytometry data were generated using the t-distributed stochastic neighbor embedding (tSNE) algorithm (van der Maaten and Hinton, 2008). tSNE is a non-linear dimensionality reduction method that optimally places cells with similar expression levels near to each other and cells with dissimilar expression levels further apart. See Supplemental Experimental Procedures for how tSNE analyses were executed.

RNA-Seq

CD4$^+$ T cells, ILC2s, and ILC3s (100,000–50 cells) were sorted from PBMCs as described above into 300 μl of RLT Lysis Buffer (QIAGEN) supplemented with 1% v/v 2-mercaptoethanol, briefly vortexed, spun down, and snap-frozen on dry ice. Cellular mRNA was then isolated and processed for RNA-seq as described previously (Trombetta et al., 2014). See Supplemental Experimental Procedures for details.

Sequencing libraries were then prepared from WTA product using Nextera XT (Illumina). After library construction, one final AMPure XP SPRI clean-up (0.8 volumes) was conducted. Library concentration and size were measured with the KAPA Library Quantification kit (KAPA Biosystems) and a TapeStation (Agilent Technologies), respectively. Finally, samples were sequenced on a NextSeq500 (30 bp paired-end reads) to an average depth of 5 million reads. See Supplemental Experimental Procedures for details on gene expression data analysis.

Statistical Analyses

We used the Mann-Whitney U-test for comparison of median values between two groups only and the Dunn's multi comparisons test to compare median values of more than two groups. The Wilcoxon matched-pairs signed rank test was used for paired testing of median values before and after antiretroviral treatment for matched samples. We used the Spearman rank correlation test to compare correlation between two parameters and reported *r*-values and p values. Statistical analyses were performed with GraphPad Prism v.6.0c (GraphPad Software).

ACCESSION NUMBERS

The accession number for the RNA-seq data reported in this paper is GEO: GSE77088.

SUPPLEMENTAL INFORMATION

Supplemental Information includes seven figures, five tables, and Supplemental Experimental Procedures and can be found with this article online at http://dx.doi.org/10.1016/j.immuni.2016.01.006.

AUTHOR CONTRIBUTIONS

H.N.K. designed and performed the study and wrote the paper. S.W.K. and A.K.S. performed RNA-seq experiments. Additional experiments were performed by J.M.M., A.W., M.C.Y., S.N., P.K., K.P., and W.A.B. tSNE analysis was by Y.S. and E.W.N. The acute infection cohort was established and coordinated by Z.N., K.D., A.M., B.D.W., and T.N., who also provided clinical specimens and clinical data. M.M., F.A., W.K., N.G., V.K., S.S.A.K., and P.G. provided clinical samples and clinical data. J.M., B.D.W., and T.N. provided intellectual input and contributed to the manuscript. A.L. provided intellectual input, contributed to the design, and wrote the paper.

ACKNOWLEDGMENTS

Funding was provided by The Danish Agency for Science, Technology and Innovation (grant #12-132295), Lundbeck Foundation (grant #R151-2013-14624), and MAERSK Foundation (all to H.N.K.); by the Collaboration for AIDS Vaccine Discovery of the Bill and Melinda Gates Foundation and NIH grant AI067073 (both to B.D.W.); by partial support from the Bill and Melinda Gates Foundation, the International AIDS Vaccine Initiative (IAVI) (UKZNRSA1001), and the NIAID (R37AI067073); by The South African Research Chairs Initiative, an International Early Career Scientist Award from the Howard Hughes Medical Institute, and the Victor Daitz Foundation (all to T.N.); by The National Science Foundation Graduate Research Fellowship Program (NSF GRFP) (to S.W.K.); and by The Searle Scholars Program (A.K.S.). We thank Dr. Hollis Shen for extensive support during cell sorting; all "iThimba," "Gateway," "CAPRISA002/004," and "FRESH" Acute Infection Study participants; the supportive role of the CAPRISA002/004 studies; Carly G.K. Ziegler and Travis K. Hughes (from the A.K.S. lab) for help on analysis of the RNA-seq data; and NIH AIDS Reagent Program, Division of AIDS, NIAID, NIH, for $\alpha 4\beta 7$ monoclonal antibody (cat# 11718) from Dr. A.A. Ansari.

Received: August 12, 2015
Revised: October 13, 2015
Accepted: November 2, 2015
Published: February 2, 2016

REFERENCES

Abdool Karim, Q., Abdool Karim, S.S., Frohlich, J.A., Grobler, A.C., Baxter, C., Mansoor, L.E., Kharsany, A.B., Sibeko, S., Mlisana, K.P., Omar, Z., et al.; CAPRISA 004 Trial Group (2010). Effectiveness and safety of tenofovir gel, an antiretroviral microbicide, for the prevention of HIV infection in women. Science *329*, 1168–1174.

Bartemes, K.R., Kephart, G.M., Fox, S.J., and Kita, H. (2014). Enhanced innate type 2 immune response in peripheral blood from patients with asthma. J. Allergy Clin. Immunol. *134*, 671–678.e4.

Becher, B., Schlitzer, A., Chen, J., Mair, F., Sumatoh, H.R., Teng, K.W., Low, D., Ruedl, C., Riccardi-Castagnoli, P., Poidinger, M., et al. (2014). High-dimensional analysis of the murine myeloid cell system. Nat. Immunol. *15*, 1181–1189.

Boyd, A., Ribeiro, J.M., and Nutman, T.B. (2014). Human CD117 (cKit)+ innate lymphoid cells have a discrete transcriptional profile at homeostasis and are expanded during filarial infection. PLoS ONE *9*, e108649.

Brenchley, J.M., Schacker, T.W., Ruff, L.E., Price, D.A., Taylor, J.H., Beilman, G.J., Nguyen, P.L., Khoruts, A., Larson, M., Haase, A.T., and Douek, D.C. (2004). CD4+ T cell depletion during all stages of HIV disease occurs predominantly in the gastrointestinal tract. J. Exp. Med. *200*, 749–759.

Cella, M., Fuchs, A., Vermi, W., Facchetti, F., Otero, K., Lennerz, J.K.M., Doherty, J.M., Mills, J.C., and Colonna, M. (2009). A human natural killer cell subset provides an innate source of IL-22 for mucosal immunity. Nature *457*, 722–725.

Cupedo, T., Crellin, N.K., Papazian, N., Rombouts, E.J., Weijer, K., Grogan, J.L., Fibbe, W.E., Cornelissen, J.J., and Spits, H. (2009). Human fetal lymphoid tissue-inducer cells are interleukin 17-producing precursors to RORC+ CD127+ natural killer-like cells. Nat. Immunol. *10*, 66–74.

Diefenbach, A. (2013). Innate lymphoid cells in the defense against infections. Eur. J. Microbiol. Immunol. (Bp.) *3*, 143–151.

Doitsh, G., Galloway, N.L., Geng, X., Yang, Z., Monroe, K.M., Zepeda, O., Hunt, P.W., Hatano, H., Sowinski, S., Muñoz-Arias, I., and Greene, W.C. (2014). Cell death by pyroptosis drives CD4 T-cell depletion in HIV-1 infection. Nature *505*, 509–514.

Hodge, J.N., Srinivasula, S., Hu, Z., Read, S.W., Porter, B.O., Kim, I., Mican, J.M., Paik, C., Degrange, P., Di Mascio, M., and Sereti, I. (2011). Decreases in IL-7 levels during antiretroviral treatment of HIV infection suggest a primary mechanism of receptor-mediated clearance. Blood *118*, 3244–3253.

Hunt, P.W., Sinclair, E., Rodriguez, B., Shive, C., Clagett, B., Funderburg, N., Robinson, J., Huang, Y., Epling, L., Martin, J.N., et al. (2014). Gut epithelial barrier dysfunction and innate immune activation predict mortality in treated HIV infection. J. Infect. Dis. *210*, 1228–1238.

Li, H., Richert-Spuhler, L.E., Evans, T.I., Gillis, J., Connole, M., Estes, J.D., Keele, B.F., Klatt, N.R., and Reeves, R.K. (2014). Hypercytotoxicity and rapid loss of NKp44+ innate lymphoid cells during acute SIV infection. PLoS Pathog. *10*, e1004551.

Marchetti, G., Tincati, C., and Silvestri, G. (2013). Microbial translocation in the pathogenesis of HIV infection and AIDS. Clin. Microbiol. Rev. *26*, 2–18.

Mattapallil, J.J., Douek, D.C., Hill, B., Nishimura, Y., Martin, M., and Roederer, M. (2005). Massive infection and loss of memory CD4+ T cells in multiple tissues during acute SIV infection. Nature *434*, 1093–1097.

McHedlidze, T., Waldner, M., Zopf, S., Walker, J., Rankin, A.L., Schuchmann, M., Voehringer, D., McKenzie, A.N., Neurath, M.F., Pflanz, S., and Wirtz, S. (2013). Interleukin-33-dependent innate lymphoid cells mediate hepatic fibrosis. Immunity *39*, 357–371.

McKenzie, A.N., Spits, H., and Eberl, G. (2014). Innate lymphoid cells in inflammation and immunity. Immunity *41*, 366–374.

McMichael, A.J., Borrow, P., Tomaras, G.D., Goonetilleke, N., and Haynes, B.F. (2010). The immune response during acute HIV-1 infection: clues for vaccine development. Nat. Rev. Immunol. *10*, 11–23.

Monticelli, L.A., Sonnenberg, G.F., Abt, M.C., Alenghat, T., Ziegler, C.G.K., Doering, T.A., Angelosanto, J.M., Laidlaw, B.J., Yang, C.Y., Sathaliyawala, T., et al. (2011). Innate lymphoid cells promote lung-tissue homeostasis after infection with influenza virus. Nat. Immunol. *12*, 1045–1054.

Munneke, J.M., Björklund, A.T., Mjösberg, J.M., Garming-Legert, K., Bernink, J.H., Blom, B., Huisman, C., van Oers, M.H., Spits, H., Malmberg, K.J., and Hazenberg, M.D. (2014). Activated innate lymphoid cells are associated with a reduced susceptibility to graft-versus-host disease. Blood *124*, 812–821.

Ndhlovu, Z.M., Kamya, P., Mewalal, N., Kløverpris, H.N., Nkosi, T., Pretorius, K., Laher, F., Ogunshola, F., Chopera, D., Shekhar, K., et al. (2015). Magnitude and kinetics of CD8+ T cell activation during hyperacute HIV infection impact viral set point. Immunity *43*, 591–604.

Perry, J.S., Han, S., Xu, Q., Herman, M.L., Kennedy, L.B., Csako, G., and Bielekova, B. (2012). Inhibition of LTi cell development by CD25 blockade is associated with decreased intrathecal inflammation in multiple sclerosis. Sci. Transl. Med. *4*, 145ra106.

Petrovas, C., Mueller, Y.M., Dimitriou, I.D., Bojczuk, P.M., Mounzer, K.C., Witek, J., Altman, J.D., and Katsikis, P.D. (2004). HIV-specific CD8+ T cells exhibit markedly reduced levels of Bcl-2 and Bcl-xL. J. Immunol. *172*, 4444–4453.

Rapaport, F., Khanin, R., Liang, Y., Pirun, M., Krek, A., Zumbo, P., Mason, C.E., Socci, N.D., and Betel, D. (2013). Comprehensive evaluation of differential gene expression analysis methods for RNA-seq data. Genome Biol. *14*, R95.

Reeves, R.K., Rajakumar, P.A., Evans, T.I., Connole, M., Gillis, J., Wong, F.E., Kuzmichev, Y.V., Carville, A., and Johnson, R.P. (2011). Gut inflammation and indoleamine deoxygenase inhibit IL-17 production and promote cytotoxic potential in NKp44+ mucosal NK cells during SIV infection. Blood *118*, 3321–3330.

Robinette, M.L., Fuchs, A., Cortez, V.S., Lee, J.S., Wang, Y., Durum, S.K., Gilfillan, S., and Colonna, M.; Immunological Genome Consortium (2015). Transcriptional programs define molecular characteristics of innate lymphoid cell classes and subsets. Nat. Immunol. *16*, 306–317.

Sanchez, J.L., Hunt, P.W., Reilly, C.S., Hatano, H., Beilman, G.J., Khoruts, A., Jasurda, J.S., Somsouk, M., Thorkelson, A., Russ, S., et al. (2015). Lymphoid fibrosis occurs in long-term nonprogressors and persists with antiretroviral therapy but may be reversible with curative interventions. J. Infect. Dis. *211*, 1068–1075.

Schuetz, A., Deleage, C., Sereti, I., Rerknimitr, R., Phanuphak, N., Phuang-Ngern, Y., Estes, J.D., Sandler, N.G., Sukhumvittaya, S., Marovich, M., et al.; RV254/SEARCH 010 and RV304/SEARCH 013 Study Groups (2014). Initiation of ART during early acute HIV infection preserves mucosal Th17 function and reverses HIV-related immune activation. PLoS Pathog. *10*, e1004543.

Sonnenberg, G.F., Monticelli, L.A., Alenghat, T., Fung, T.C., Hutnick, N.A., Kunisawa, J., Shibata, N., Grunberg, S., Sinha, R., Zahm, A.M., et al. (2012). Innate lymphoid cells promote anatomical containment of lymphoid-resident commensal bacteria. Science *336*, 1321–1325.

Spencer, S.P., Wilhelm, C., Yang, Q., Hall, J.A., Bouladoux, N., Boyd, A., Nutman, T.B., Urban, J.F., Jr., Wang, J., Ramalingam, T.R., et al. (2014). Adaptation of innate lymphoid cells to a micronutrient deficiency promotes type 2 barrier immunity. Science *343*, 432–437.

Spits, H., Artis, D., Colonna, M., Diefenbach, A., Di Santo, J.P., Eberl, G., Koyasu, S., Locksley, R.M., McKenzie, A.N., Mebius, R.E., et al. (2013). Innate lymphoid cells–a proposal for uniform nomenclature. Nat. Rev. Immunol. *13*, 145–149.

Stacey, A.R., Norris, P.J., Qin, L., Haygreen, E.A., Taylor, E., Heitman, J., Lebedeva, M., DeCamp, A., Li, D., Grove, D., et al. (2009). Induction of a striking systemic cytokine cascade prior to peak viremia in acute human immunodeficiency virus type 1 infection, in contrast to more modest and delayed responses in acute hepatitis B and C virus infections. J. Virol. *83*, 3719–3733.

Tait Wojno, E.D., and Artis, D. (2012). Innate lymphoid cells: balancing immunity, inflammation, and tissue repair in the intestine. Cell Host Microbe *12*, 445–457.

Teunissen, M.B., Munneke, J.M., Bernink, J.H., Spuls, P.I., Res, P.C., Te Velde, A., Cheuk, S., Brouwer, M.W., Menting, S.P., Eidsmo, L., et al. (2014). Composition of innate lymphoid cell subsets in the human skin: enrichment of NCR(+) ILC3 in lesional skin and blood of psoriasis patients. J. Invest. Dermatol. *134*, 2351–2360.

Trombetta, J.J., Gennert, D., Lu, D., Satija, R., Shalek, A.K., and Regev, A. (2014). Preparation of single-cell RNA-seq libraries for next generation sequencing. Curr. Protoc. Mol. Biol. *107*, 1–17.

van der Maaten, L., and Hinton, G. (2008). Visualizing data using t-SNE. J. Mach. Learn. Res. *9*, 2579–2605.

Veazey, R.S., DeMaria, M., Chalifoux, L.V., Shvetz, D.E., Pauley, D.R., Knight, H.L., Rosenzweig, M., Johnson, R.P., Desrosiers, R.C., and Lackner, A.A. (1998). Gastrointestinal tract as a major site of CD4+ T cell depletion and viral replication in SIV infection. Science *280*, 427–431.

Xu, H., Wang, X., Lackner, A.A., and Veazey, R.S. (2015). Type 3 innate lymphoid cell depletion is mediated by TLRs in lymphoid tissues of simian immunodeficiency virus-infected macaques. FASEB J. *29*, 5072–5080.

Zeng, M., Southern, P.J., Reilly, C.S., Beilman, G.J., Chipman, J.G., Schacker, T.W., and Haase, A.T. (2012). Lymphoid tissue damage in HIV-1 infection depletes naïve T cells and limits T cell reconstitution after antiretroviral therapy. PLoS Pathog. *8*, e1002437.

Zhang, Z., Cheng, L., Zhao, J., Li, G., Zhang, L., Chen, W., Nie, W., Reszka-Blanco, N.J., Wang, F.S., and Su, L. (2015). Plasmacytoid dendritic cells promote HIV-1-induced group 3 innate lymphoid cell depletion. J. Clin. Invest. *125*, 3692–3703.